View metadata, citation and similar papers at core.ac.uk
brought to you by CORE
provided by HZB Repository

Raman and Photoreflectance Study of $Cu(In,Ga)S_2$ Films and Solar-Cells

S. THEODOROPOULOU[1], D. PAPADIMITRIOU[1], S. BAKEHE[2], R. KLENK[2], M.CH. LUX-STEINER[2]

[1]Department of Physics
National Technical University of Athens
GR-15780 Athens
GREECE

[2]Department SE2, Heterogeneous Material Systems,
Hahn-Meitner Institut
Glienickerstr. 100, D-14109 Berlin
GERMANY
http://www.hmi.de

Abstract: - The structural and optical properties of $CuIn_{1-x}Ga_xS_2$ (CIGS), $CdS/CuIn_{1-x}Ga_xS_2$, and $ZnO/CdS/CuIn_{1-x}Ga_xS_2$ polycrystalline films, with applications in photovoltaics, were studied by Raman and Photoreflectance (PR) spectroscopy for two different compositions, [Ga]/([In]+[Ga]) =0.04 and 0.12, of the $CuIn_{1-x}Ga_xS_2$ absorber. The energy band gap of the absorber film was determined by fitting the PR-spectra with a third derivative functional form. Moreover, the thickness of the film was calculated from the interference fringes observed in the PR-spectra below band gap energy. Raman scattering was excited by the 514.5nm line of Ar^+-laser and the 647.1nm line of Kr^+-laser. The Raman spectra of the absorber films consist of phonon-modes assigned to $CuInS_2$, $CuGaS_2$ and CuS. The results of the present study are discussed together with the results of SEM and XRD studies of the films and the results of electrical measurements performed on solar cells based on the CIGS absorbers.

Key-Words: - $CuInS_2$, $CuIn_{17-x}Ga_xS_2$, thin film solar cells, Photoreflectance, Raman.

1 Introduction

$CuInS_2$ (CIS) is the most-promising wide-gap chalcopyrite absorber for thin-film solar cells. Its direct band gap E_g of 1.5 eV is suitable for single-junction cells. A wider band gap is desirable for the top cell in tandem configurations and can be achieved by incorporating gallium [1]. $Cu(In,Ga)S_2$ (CIGS)-based solar cells exhibit various benefits such as improved adhesion and open circuit voltage as well as higher flexibility in the choice of process parameters, as reported by several authors [2-5].

It has been shown that the kinetics of film formation in the two-step process lead to an intermediate bi-layer structure of $CuInS_2$ on $CuGaS_2$ and that the [Ga]/[In] ratio only partly homogenises by interdiffusion during later stages of sulphurisation [6]. Hence, the gallium concentration is high close to the back contact and decreases towards the film surface. This leads to an inherent grading of the band gap. The two-step process can be modified [7] to give a more uniform distribution of Ga in the active layer. However, the maximum achievable band gap in the active region of the cell is limited to approximately 1.6 eV which corresponds to a x=([Ga]/([In]+[Ga]) ratio of approximately 0.10.

The scope of this paper is to study the properties of $CuIn_{1-x}Ga_xS_2$-based films with two different x=[Ga]/([In]+[Ga]) ratios (0.04 and 0.12) and to evaluate the performance of solar cells based on these films. The absorber with x=0.12 is already at the upper limit of the quaternary that can lead to good quality CIGS solar cells with maximum widened energy gap, while the one with x=0.04 is expected to give results very close to the ternary CIS chalcopyrite.

2 Experimental

The investigated samples consist of a soda lime glass coated with sputtered Mo back contact as a substrate, a $CuIn_{1-x}Ga_xS_2$ (CIGS) absorber layer, a CdS buffer layer, a ZnO window and an Al/Ni grid as front contact [7,8]. The $CuIn_{1-x}Ga_xS_2$ absorber layers are deposited using two different two-stage sequences: for the lower band gap absorber (x=0.04), evaporation takes place with constant rate at constant substrate temperature, while for the absorber with x=0.12, evaporation of Cu (below stoichoiometry), In, Ga, and S at lower substrate temperature (typically 250 ^oC) is followed by evaporation of Cu and S at higher (typically 500 ^oC) substrate temperature. The buffer layer is deposited by chemical bath, the window layer is formed by sputtering and the front contact is evaporated [8]. All films were slightly Cu-rich after preparation and the secondary CuS phase formed on the absorber surface was removed by KCN-etching. Further details on the preparation and structural characterization of the films and solar cells are described elsewhere [7].

$CuInS_2$ polycrystalline films were also prepared using a procedure similar to the one applied in the preparation of the higher band gap quaternary chalcopyrite. The only difference was the absence of Cu in the first stage of the process.

The PR-spectra of the $CuIn_{1-x}Ga_xS_2$ (CIGS) and $CdS/CuIn_{1-x}Ga_xS_2$ films were excited at 20K by the 488 nm (or 457.9 nm) line of an argon (Ar^+) laser as modulation source. The PR-spectra of the $ZnO/CdS/CuIn_{1-x}Ga_xS_2$ films were excited at 20K by the 351 nm line of a Krypton (Kr^+) laser. A Xenon (or a Halogen) lamp was used as a light source. The reflected beam was spectrally analyzed by a single-grating monochromator (SPEX 1704) and detected by a Si-diode. The detected light was amplified by lock-in techniques. For the low temperature measurements, the samples were cooled down to 20K in a closed-cycle He-cryostat.

The Raman spectra of the $CuIn_{1-x}Ga_xS_2$ (CIGS), $CdS/CuIn_{1-x}Ga_xS_2$, and $ZnO/CdS/CuIn_{1-x}Ga_xS_2$ polycrystalline films were measured at room temperature using the 514.5nm line of an Ar^+-laser and the 647.1nm line of a Kr^+-laser as excitation source. The scattered light was spectrally analyzed by a double grating monochromator and detected by a GaAs-PMT detector.

3 Results and discussion

In Fig. 1, the PR-spectra of the $CuIn_{1-x}Ga_xS_2$ (CIGS) samples (x=0, 0.04, and 0.12) at 20 K are shown. The room temperature PR-spectra could not be evaluated due to their low intensity to noise ratio and they will not be further discussed.

The structure of the fundamental absorption edge of chalcopyrites is well understood [9]. These crystals are semiconductors with a direct fundamental band gap at the Brillouin-zone centre Γ. The threefold valence-band maximum is composed of three nondegenerate states, giving rise to three transitions called E_a, E_b, E_c from smaller to larger energy (Fig. 2). Experimental measurements of these transition energies and their selection rules allow us to determine the symmetry of the three valence states and to calculate the crystal-field (Δ_{cf}) and the spin-orbit (Δ_{so}) parameters, using the quasi-cubic model [10]. Starting from the threefold-degenerate Γ_{15} state in zinc blende, the introduction of a tetragonal crystal field gives rise to one Γ_4 plus a twofold-degenerate Γ_5 level. Spin-orbit interaction further splits the Γ_5 levels into Γ_7 and Γ_6 and the selection rules are relaxed.

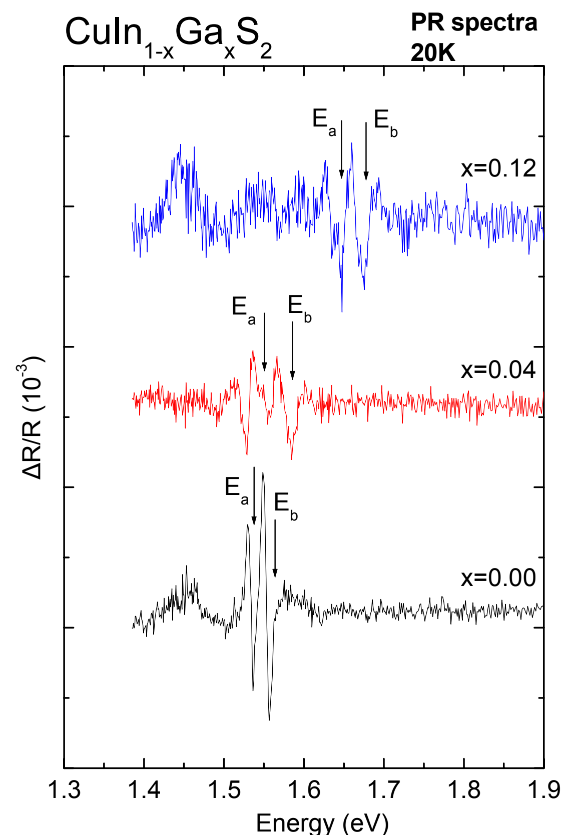

Fig.1. PR-spectra of $CuIn_xGa_{1-x}S_2$ (x=0, 0.04, and 0.12).

In $CuInS_2$ (CIS), with a small distortion from the cubic symmetry, the A and B peaks are so close that they are never resolved at room temperature ($\Delta_{cf}>0$) [11]. However, Tell et al. [12], by comparing the electro- (ER) and photoreflectance (PR) spectra with reflectance spectra, concluded that the dominating mechanism for $CuInS_2$ at 2 K is the change in the dielectric functions of two excitonic transitions. Low-temperature studies of exciton reflectivity and photoreflectance have failed to locate a third valence band in any of the studied sulphides, CIS included [13]. The PR spectra of $CuInS_2$ single crystals below 200 K consist of two well-resolved peaks related to the fundamental transition E_0 and the transition involving spin-orbit splitting $E_0+\Delta_0$ [14]. In general, in the low temperature PR spectra, only E_a- and E_b- transitions are expected to appear [13]. The two bands observed in the PR spectra of the absorbers in Fig.1 are, thereafter, attributed to the E_a- and E_b- excitonic transitions.

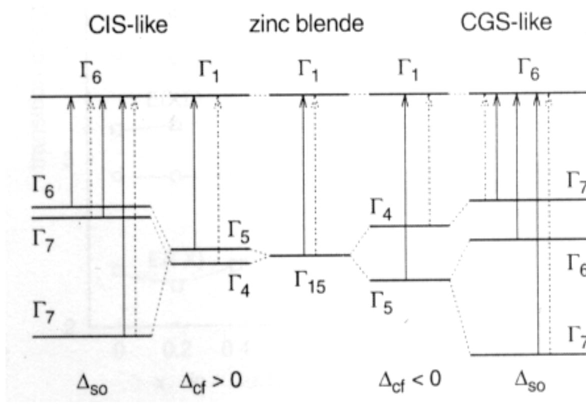

Fig.2 Schematic evolution of the energy states at the band gap of chalcopyrite starting from a zinc blende-like gap without spin-orbit coupling.

In the photoreflectance spectra, the modulation of the optical constants is produced by the periodic cancellation of the built-in surface field resulting from the photoexcitation by the laser beam. Basically, the PR spectrum can be described by a third derivative line shape [15] similar to the case of electroreflectance.

The fitting of the PR spectra using a Third Derivative Functional Form (TDFF) gives the positions of the fundamental band gap energies of the ternary and two quaternary polycrystalline absorbers. For the ternary $CuInS_2$, the energies of the E_a and the E_b bands are: E_a =(1.533±0.001) eV and E_b =(1.552±0.001) eV. For the quaternary absorbers $CuIn_{1-x}Ga_xS_2$ with x=0.04 and 0.12, we obtain E_a=(1.532±0.001) eV, E_b=(1.580±0.002) eV and E_a=(1.651±0.002) eV, E_b=(1.672±0.002) eV, respectively. The fitted values (Fig. 3) are in good agreement with the linear dependence of the energy band gap on the Ga-fraction reported in experimental PR studies of quaternary chalcopyrites [16].

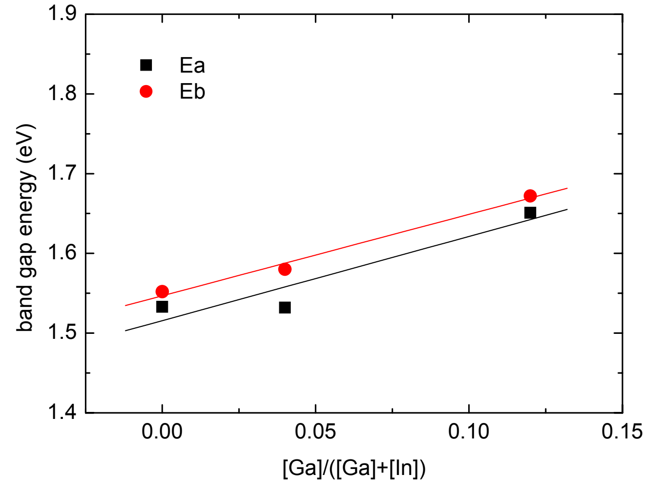

Fig.3. Compositional dependence of the E_a and E_b transition energies.

The PR-spectra of the $CuIn_{1-x}Ga_xS_2$ layer with the deposited CdS buffer layer on top of the chalcopyrite absorber at 20 K are shown in Fig. 4. Apart from the absorber bands, a band assigned to CdS is observed on the high energy side of these spectra. The band gap energy of the E_a-transition in CdS was found to be E_a=(2.501±0.002) and (2.487±0.007) eV for x=0.04 and 0.12, respectively, which is in good agreement with the values known from the literature [17]. These spectra exhibit a number of interference fringes at energies below the band gap energy. Similar interference fringes are also present in the reflectance spectra of the $CuIn_{1-x}Ga_xS_2$ absorbers, as demonstrated in Fig. 5. The fringes are originating from the interference of light beams reflected on the front and back face of the absorber layer. The interferences influence the PR absorber line shapes: the E_a gap is shadowed, while the E_b gap is up-shifted to E_b=(1.575±0.004) eV and (1.681±0.008) eV for x=0.04 and 0.12, respectively.

The interference fringes observed in the reflectance spectra (Fig. 5) can be used to calculate the absorber thickness using a relationship derived in ref. [18]:

$$t = \frac{N\,\lambda_1\lambda_2}{2(\lambda_1-\lambda_2)\left(n^2-\sin^2\theta\right)^{1/2}} \qquad (1)$$

where t is the layer thickness, n is the refractive index of the layer, θ is the angle of incidence, λ_1, λ_2 are the start and end wavelength ($\lambda_1 > \lambda_2$), respectively, and N is the number of fringes between λ_1 and λ_2.

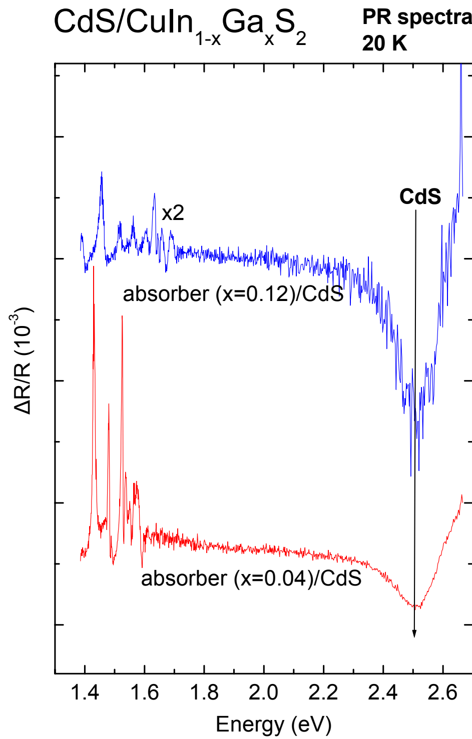

Fig.4. PR-spectra of $CdS/CuIn_{1-x}Ga_xS_2$ (x=0.04 and 0.12).

For the calculation of the absorber thickness, the refractive index of the ternary $CuInS_2$ is used [19], since the refractive index of the quaternary $CuIn_{1-x}Ga_xS_2$ is not known. In ref. [20], two different values of n corresponding to the start- and end-wavelength of the scanned region were chosen. In the present work, the wavelength dispersion of n has been taken into account by choosing a value in the middle of the scanned spectral region: n=2.87 at 1.5 eV. By adding Ga into $CuInS_2$, the refractive index of the quaternary compound is lowered. The refractive index of pure $CuGaS_2$ is n=2.59 at 1.5 eV [19]. However, addition of 4%-12% Ga does not significantly changes the refractive index of the ternary. In fact, the refractive indices of the quaternary films studied are almost the same as the refractive index of $CuInS_2$ due to the small gallium content of the films (≤12%). The calculated thickness for the non-etched absorbers with x=0.04 and 0.12 are 3.8 and 3.9 μm, respectively. According to the scanning electron micrographs (SEM) in Fig. 6, the films appear to be compact with grain sizes in the order of one μm. Prior to etching, the film is covered homogenously with CuS, which is important in view of the growth assistance provided by this phase [7].

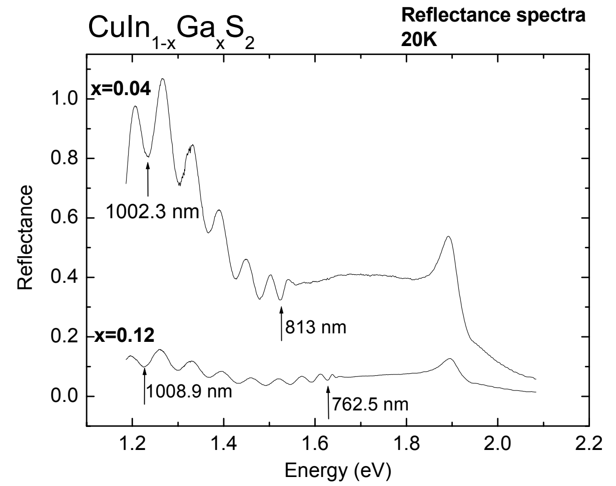

Fig. 5. Reflectance spectra of $CuIn_xGa_{1-x}S_2$ (x= 0.04 and 0.12).

The SEM data of the etched absorbers give a film thickness of about 3 μm, for both Ga fractions. Using equation (1) for t=3 μm, we obtain a refractive index of 3.66 and 3.71 for the absorber films with x=0.04 and 0.12, respectively. This discrepancy between SEM and PR results on the thickness determination is tentatively attributed to In_2S_3 and GaS secondary phases within the film [7]. CuS segregates on the surface, as stated in the experimentals, and can be removed by KCN-etching. PR-spectroscopy detects only a mean value of the refractive index of the layer (the so called *effective* refractive index).

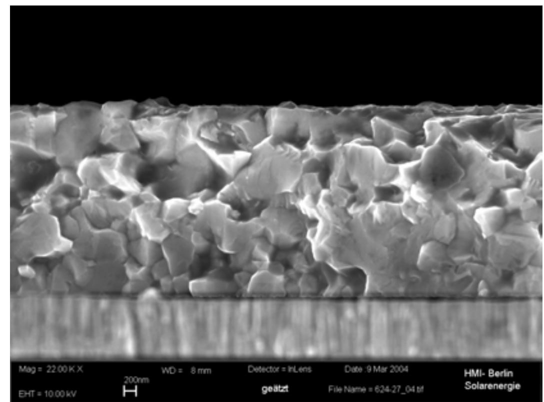

Fig.6. Scanning electron micrograph of a $CuIn_{1-x}Ga_xS_2$ film with x=0.04 (cross-section).

The PR-spectrum of the $ZnO/CdS/CuIn_{1-x}Ga_xS_2$ film with x=0.12 at 20 K is shown in Fig. 7. In the

low energy region, the E_a-band of the absorber layer is observed, while the narrow band at higher energies is due to the polycrystalline ZnO layer deposited on top of the absorber and the buffer layer. The band gap energy of ZnO is calculated to (3.367±0.001) eV, in agreement with values reported in the literature [21, 22].

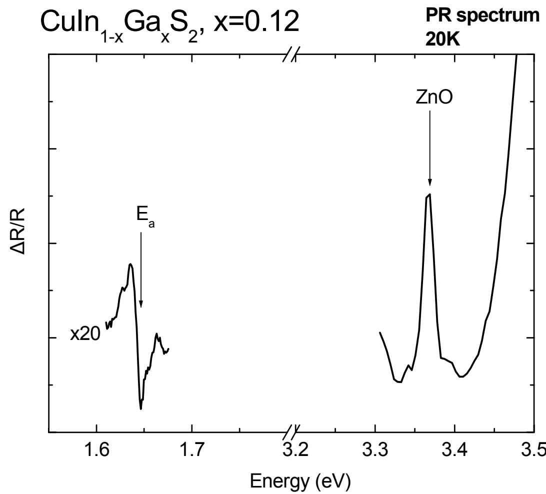

Fig.7. Photoreflectance spectrum of ZnO/CdS/ $CuIn_xGa_{1-x}S_2$ with x= 0.12.

In Fig. 8, the Raman spectra of the $CuIn_{1-x}Ga_xS_2$, $CdS/CuIn_{1-x}Ga_xS_2$, and $ZnO/CdS/CuIn_{1-x}Ga_xS_2$ samples with x=0.04, excited by two different laser beams, the 514.5nm line of an Ar^+-laser and the 647.1nm line of a Kr^+-laser, are shown. The Raman spectra of the $CuIn_{1-x}Ga_xS_2$, $CdS/CuIn_{1-x}Ga_xS_2$ and $ZnO/CdS/CuIn_{1-x}Ga_xS_2$ samples with x=0.12 are presented in Fig. 9.

The Raman spectra of the absorbers exhibit peaks that can be attributed to the phonon modes of the ternary $CuInS_2$ and $CuGaS_2$ chalcopyrites and to the modes of the CuS secondary phase that is formed during the preparation process. The Raman-band frequencies were determined by fitting the Raman spectra with Lorentzians. In Figs. 8(a) and 9(a), the two weak peaks at 262 and 292 cm^{-1} are assigned to the E(TO)-mode of $CuGaS_2$ and to the A_1-mode of $CuInS_2$, respectively. An intense peak at 300 cm^{-1}, in the spectra of the $CdS/CuIn_{1-x}Ga_xS_2$ and $ZnO/CdS/CuIn_{1-x}Ga_xS_2$ layers excited by the 514.5 nm (2.4 eV) laser line, is attributed to the first order A_1 (LO) mode of the CdS buffer layer [23]. The phonon mode at 600 cm^{-1}, has twice the frequency of the mode at 300 cm^{-1} and is, therefore, assigned to the second order Raman scattering (RS) of CdS. The high intensity of these peaks is due to the resonant Raman scattering of CdS; its energy band gap of 2.5 eV [17] is close to the excitation energy of 2.4 eV. The mode assignment of the Raman spectra of $CuIn_{1-x}Ga_xS_2$, $CdS/CuIn_{1-x}Ga_xS_2$ and $ZnO/CdS/CuIn_{1-x}Ga_xS_2$ layers with x=0.04, given in Figs. 8(b) and 9(b), is as follows: the peak at 63 cm^{-1} is assigned to the E(TO)-mode of $CuInS_2$, the peak at 95 cm^{-1} to the B_2(TO or LO)-mode of $CuGaS_2$, the peak at 234 cm^{-1} to the B_2(TO)-mode of $CuInS_2$, the peak at 262 cm^{-1} to the E(TO)-mode of $CuGaS_2$, the peak at 292 cm^{-1} to the A_1-mode of $CuInS_2$, the peak at 355 cm^{-1} to the E(LO)-mode of $CuGaS_2$, the peak at 472 cm^{-1} to the A_1-mode of CuS [24] and the peak at 524 cm^{-1} to the second order of the E(TO)-mode of $CuGaS_2$ [25]. No significant shift of the Raman band frequencies could be observed, as expected by substitution of In by Ga in $CuInS_2$ and formation of $CuIn_{1-x}Ga_xS_2$. This is partially due to the small Ga content of the absorber layers ($x \leq 0.12$) and partially due to the formation of a gradient composition layer (for x=0.04) with $CuInS_2$ on the top, $CuGaS_2$ at the bottom, and $CuIn_{1-x}Ga_xS_2$ in between, as has been shown by depth profiling [26]. In fact, previously published results of XRD studies on the same samples [7] have confirmed the presence of a quaternary chalcopyrite phase.

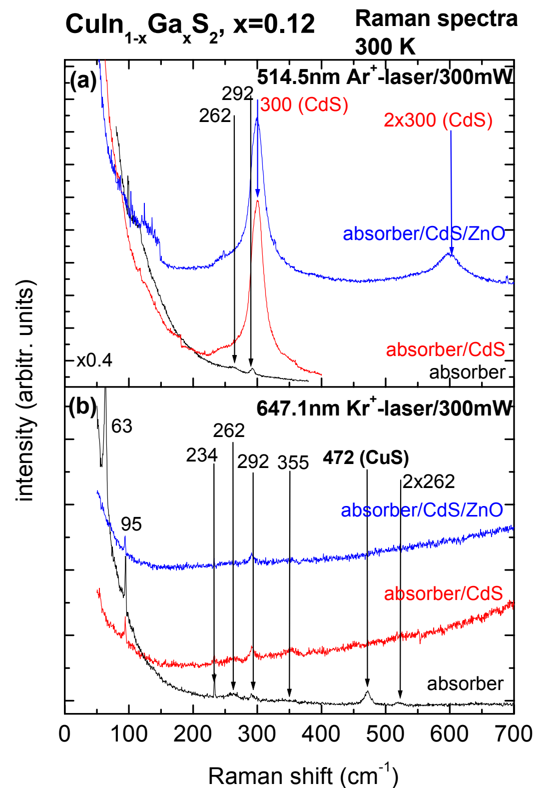

Fig.8. Raman spectra of the $CuIn_{1-x}Ga_xS_2$, $CdS/CuIn_{1-x}Ga_xS_2$, and ZnO/CdS/ $CuIn_{1-x}Ga_xS_2$ layers with x=0.12, excited by two different laser beams.

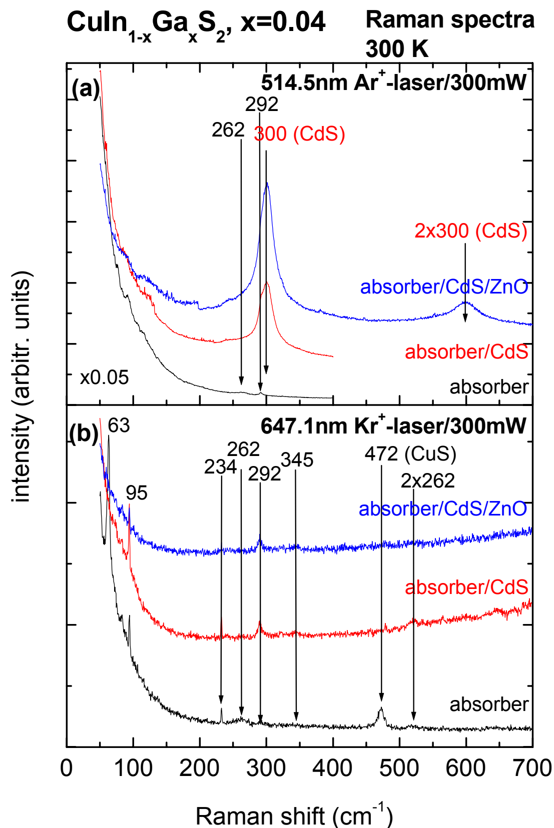

Fig.9. Raman spectra of the $CuIn_{1-x}Ga_xS_2$, $CdS/CuIn_{1-x}Ga_xS_2$, and $ZnO/CdS/CuIn_{1-x}Ga_xS_2$ samples with x=0.04, excited by two different laser beams.

The electrical measurements performed on solar cells based on the CIGS absorbers show that open circuit voltages increase up to 800 mV with increasing absorber band gap. On the other hand, comparison of fill factors and quantum efficiencies of the two different CIGS-solar cells under study reveals [7], [27] that, while the band gap is raised (CIS/x=0, 1.5eV/11.4%, CIGS/x=0.04, 1.53eV /12.3%, CIGS/x=0.12, 1.65eV/10.1%, CGS/x=1, 1.68eV/8.3%), the efficiency drops back. However, the CIGS cells show a better performance than CGS based cells with a comparable band gap, though the latter have been under development for many years.

4 Conclusions

$CuIn_{1-x}Ga_xS_2$ (CIGS), $CdS/CuIn_{1-x}Ga_xS_2$, and $ZnO/CdS/CuIn_{1-x}Ga_xS_2$ polycrystalline films, with applications in photovoltaics, were studied by Raman and Photoreflectance (PR) spectroscopy for two different compositions (Ga/(In+Ga) =0.04 and 0.12) of the $CuIn_{1-x}Ga_xS_2$ absorber. The band gap energies of the absorber layers as well as those of the buffer and the ZnO layer were determined by fitting the PR-spectra. Moreover, the absorber thickness was obtained from the interference fringes of the PR-spectra below band gap energy. The phonon modes observed in the Raman spectra were attributed to the ternary compounds $CuInS_2$ and $CuGaS_2$.

Acknowledgements

This project is co-funded by the European Social Fund (75%) and National Resources (25%).

References:

[1] R.Klenk, S.Bakehe, R.Kaigawa, A.Neisser, J.Reiβ, M.Ch.Lux-Steiner, Optimizing the open-circuit voltage of $Cu(In,Ga)S_2$ solar cells-design and analysis, *Thin Solid Films*, Vol. 451-452, 2004, pp. 424-429.

[2] T.Watanabe, M.Matsui, Improved Efficiency of $CuInS_2$-based Solar Cells without Potassium Cyanide Process, *Japanese Journal of Applied Physics,* Vol.38, 1999, pp. L1379-L1381.

[3] I.Hengel, R.Klenk, E.Garcia Villora, M.Ch.Lux-Steiner, in: J.Shmid, H.A.Ossenbrink, P.Helm, H.Ehmann, E.D.Dunlop (Eds.), *Proceedings of the 2nd World Conference On Photovoltaic Solar Energy Conversion*, Vienna, Austria, July 6-10, 1998, European Communities, Report EUR 18656 EN, 1999, 545.

[4] N.G.Dhere, S.R.Ghorgadi, in: R.Noufi, R.W.Birkmire, D.Lincot, H.W.Schock (Eds.), II-VI Compound Semiconductor Photovoltaic Materials, MRS Spring Meeting, Symposium H, San Francisco, U.S.A., April 16-20, 2001, Materials Research Society Symposium Proceeding 668 (2001) H3.4.1.

[5] T.Ohashi, Y.Hashimoto, K.Ito, *Solar Energy Materials and Solar Cells*, Solar cells with $Cu(In_{1-x}Ga_x)S_2$ thin films prepared by sulfurization Vol.67, 2001, pp. 225-230.

[6] A. Neisser, J.Alvarez-Garcia, L.Calvo-Barrio, R.Klenk, T.W.Matthes. I.Luck, M.Ch.Lux-Steiner, in: R. Noufi, R.W. Birkmire, D. Lincot, H.W. Schock (Eds.), II-VI Compound Semiconductor Photovoltaic Materials, MRS Spring Meeting, Symposium H, San Fransisco, U.S.A., April 16-20, 2001, Materials Research Society Symposium Proceeding 668 (2001) H1.3.1.

[7] R.Kaigawa, A.Neisser, R.Klenk, M.Ch.Lux-Steiner, Improved Performance of thin film solar cells based on $Cu(In,Ga)S_2$, *Thin Solid Films*, Vol.415, 2002, pp. 266-271.

[8] R. Henninger, W. Brumm. J. Bruns, J.Klaer, D. Braünig, Characterization of $CdS/CuInS_2$ Heterostructures by Electroreflectance and Photoreflectance Spectroscopy, *14th European Photovoltaic Solar Energy Conference*, Spain, 1997.
[9] J.L.Shay, J.H.Wernick, Ternary Chalcopyrites Semiconductors: Growth, Electronic Properties, and Applications, Pergamon, Oxford, 1975.
[10] J.J.Hopfield, *Journal of Physics and Chemistry of Solids*, Fine structure in the optical absorption edge of anisotropic crystals, Vol.15, No.1-2, 1960, pp. 97-107.
[11] M.I.Alonso, M.Garriga, C.A.Durante Rincón, E.Hernández, M.León, Optical functions of chalcopyrite $CuGa_xIn_{1-x}Se_2$ alloys, *Applied Physics A*, Vol.A74, 2002, pp. 659-664.
[12] B.Tell, J.L.Shay, H.M.Kasper, Electrical Properties, Optical Properties, and Band Structure of $CuGaS_2$ and $CuInS_2$, *Physical Review B,* Vol.4, 1971, pp. 2463-2471.
[13] J.L.Shay, B.Tell, H.M.Kasper, L.M.Shiavone, p-d Hybridization of the Valence Bands of I-III-VI_2 Compounds, *Physical Review B*, Vol.5, No.12, 1972, pp. 5003-5005.
[14] T.M.Hsu, J.S.Lee, H.L.Hwang, Photoreflectance of sulfur-annealed copper indium disulfide, *Journal of Applied Physics*, Vol. 68, No. 1, 1990, pp. 283-287.
[15] D.E.Aspnes, Schottky-barrier electroreflectance of Ge: Nondegenerate and orbitally degenerate critical points, *Physical Review B,* Vol.12, No.6, 1975, pp. 2297-2310.
[16] H.Metzner, J.Cieslak, J.Eberhardt, Th.Hahn, M.Müller, U.Kaiser, A.Chuvilin, U.Reislöhner, W.Witthuhn, R.Goldhahn, F.Hudert, J.Kraüβlich, Epitaxial $CuIn_{(1-x)}Ga_xS_2$ on Si(111): A perfectly lattice-matched system for $x \approx 0.5$, *Applied Physics Letters*, Vol.83, No.8, 2003, pp. 1563-1565.
[17] S.Ninomiya, S.Adachi, Optical properties of wurtzite CdS, *Journal of Applied Physics,* Vol.78, No.2, 1995, pp. 1183-1190.
[18] E.A.Corl, H.Wimpfheimer, Thickness Measurement of Silicon Dioxide Layers by Ultraviolet-Visible Interference Method, *Solid-State Electronics,* Vol.7, Pergamon Press, 1964, pp.755-761.
[19] M.I.Alonso, K.Wakita, J.Pascual, M.Garriga, N.Yamamoto, Optical functions and electronic structure of $CuInSe_2$, $CuGaSe_2$, $CuInS_2$, and $CuGaS_2$, *Physical Review B,* Vol.63, 2001, pp. 075203-1-13.
[20] M.J.Sun, Refractive-index dispersion of garnet films derived from accurate measurement of film thickness, *Applied Physics Letters,* Vol.33, No.4, 1978, pp.291-293.
[21] Y.Zhang, G.Du, X.Yang, B.Zhao, Y.Ma, T.Yang, H.C.Ong, D.Liu, S.Yang, Effect of annealing on ZnO thin films grown on (001) silicon substrate by low-pressure metalorganic chemical vapour deposition, *Semiconductor Science and Technology,* Vol.19, 2004, pp. 755-758.
[22] K.Thonke, Th.Gruder, N.Teofilov, R.Schönfelder, A.Wang, R.Sauer, Donor-acceptor pair transitions in ZnO substrate material, *Physics B*, Vol.308-310, 2001, pp. 945-948.
[23] E. Boone and C.Shannon, Properties of Ultrathin Electrodeposited CdS Films Probed by Resonance Raman Spectroscopy and Photoluminescence, *Journal of Physical Chemistry,* Vol.100, 1996, pp. 9480-9484.
[24] Sheng-Yue Wang, Wei Wang, Zu-Hong Lu, Asynchronous-pulse ultrasonic spray pyrolysis deposition of Cu_xS (x=1,2) thin films, *Materials Science and Engineering,* Vol. B103, 2003, pp. 184-188.
[25] F.W.Ohrendorf, H. Haeuseler, Lattice Dynamics of Chalcopyrite Type Compounds. Part I. Vibrational Frequences, *Crystal Research and Technology,* Vol.34, No.3, 1999, pp. 339-349.
[26] A.Neisser, I.Hengel, R.Klenk, Th.W.Matthes, J.Alvarez-Garcia, A.Perez-Rodriguez, A.Romano-Rodriguez, M.Ch.Lux-Steiner, Effect of Ga incorporation in sequentially prepared $CuInS_2$ thin film absorbers, *Solar Energy Materials and Solar Cells,* Vol.67, 2001, pp.97-104.
[27] V.Nadenau, D.Hariskos, H.W.Schock, in: H.A.Ossenbrink, P.Helm, H.Ehmann (Eds.), Proceedings of the 14th European Photovoltaic Solar Energy Conference, Barcelona, Spain, June 30-July 4, 1997, H.S.Stephens & Associates, Bedford, UK, 1997, 1250.